Energy, Exergy analysis and performance evaluation of a vacuum evaporator for solar thermal power plant Zero Liquid Discharge Systems

M. Akbari Vakilabadi[1] · M. Bidi[1] · A. F. Najafi[2] · Mohammad Hossein Ahmadi[3]

Abstract

Water scarcity and environmental impacts of blowdown within steam power plants are among the important growing concerns. In order to solve these problems, applying a zero liquid discharge (ZLD) system for treating the brine of the power plants and reusing this water is crucial. In this study, the process of a ZLD system is evaluated by using energy and exergy analyses. The ZLD system was designed to recover brines to demineralize water, which consists of four main parts including vacuum evaporator, roots pump, heat exchanger, and circulation pump. The effects of the dimensional and operating parameters on the freshwater flow rate, exergy efficiency, and the consumption power are investigated. When volume of the evaporator is 7 m^3, with increase in total evaporation time from 1 to 3 h, total power consumption decreased from 106.16 to 99.52 kW h and freshwater production reduced from 5914.62 to 2048.52 L h^{-1}. The amount of produced freshwater flow rate is independent of the recirculating flow rate and is a function of the evaporator's volume. Therefore, in volumes of 3, 5, and 7 m^3, the produced freshwater flow rate is constant at about 1300, 2200, and 3070, respectively. Also, the results showed that when increasing the concentration of the brine in the range of 2000–30,000 ppm, the flow rate of the produced freshwater decreases from 3377 to 2911 L h^{-1} and the total power consumption reduced from 113.28 to 96.42 kW h. Moreover, by increasing the volume of vacuum evaporator, freshwater flow rate rises. Increasing the freshwater flow rate has a dramatic influence on the early working cycles. Since the evaporation is a cyclic process, the exergy efficiency of the roots pump and heat exchanger improves, while the exergy efficiency of the vacuum evaporator decreases versus increasing working cycles.

Keywords Vacuum evaporator · Exergy analysis · Wastewater · Zero liquid discharge (ZLD) · Power plant blowdown

List of symbols

c	Specific heat capacity (J kg^{-1} K^{-1})
e	Specific exergy
$\dot{E}_D$	Exergy destruction (kW)
X	Salinity ratio
s	Entropy (kJ kg^{-1} K^{-1})
t	Time (s)
T	Temperature (K)
P	Pressure (kPa)
h	Enthalpy (kJ kg^{-1})
R	Gas constant (kJ kg^{-1} K^{-1})
y	Mole fraction
$\dot{Q}$	Heat transferred (kW)
$\dot{W}$	Power (kW)
m	Mass (kg)
$\dot{m}$	Flow rate (kg^{-1} s^{-1})

Greek letters

η	Isentropic efficiency

Subscripts

0	Reference ambient condition

✉ M. Bidi
  m_bidi@sbu.ac.ir

✉ Mohammad Hossein Ahmadi
  mhosein.ahmadi@shahroodut.ac.ir;
  mohammadhosein.ahmadi@gmail.com

[1] Faculty of Mechanical and Energy Engineering, Shahid Beheshti University, Tehran, Iran

[2] School of Mechanical Engineering, University of Tehran, Tehran, Iran

[3] Faculty of Mechanical Engineering, Shahrood University of Technology, Shahrood, Iran

ke	Kinetic exergy
po	Potential exergy
ph	Physical exergy
ch	Chemical exergy
is	Isentropic

Abbreviations

PHX	Preheat heat exchanger
DP	Distillate pump
CrP	Circulation pump
HX	Heat exchanger
RP	Roots pump
EV	Evaporator vacuum
FWP	Feed water pump
CFWH	Close feed water heater
OFWH	Open feed water heater
SH	Superheater
SG	Steam generator
PH	Preheater
HPT	High-pressure turbine
LPT	Low pressure turbine
RH	Reheat
ST	Storage tank
FWT	Feed water tank
PHE	Preheat exchanger
HE	Heat exchanger

Introduction

Growing urban population leads to a higher wastewater production [1, 2]. The treatment of brine streams is an appropriate solution to overcome the growing water demand [3]. Industrial processes usually make undesirable wastewater which has harmful effects on the environment [4].

In 2016, Nokoa et al. [5] analyzed a desalination system with zero liquid discharge. The system contained a hydrophobic microporous membrane module and a plastic vane. It was concluded that the system can produce 52 L day^{-1} of freshwater per one square meter of the membrane and the amount of the consumed thermal energy of the system was 11 kW m^{-2}. Naseri et al. [6] studied a transcritical CO_2 cycle by adding a near-ZLD system. The output wastewater of RO desalination was converted to beneficial products (NaCIO and H_2) with an electrolyzer. Han et al. [7] analyzed a ZLD desalination system using single- and multistage mechanical vapor compression system. They concluded that by increasing the number of stages, the consumption power of the compressor is decreased.

In recent years, using organic fuels instead of fossil fuel to reduce air pollution has been introduced as a novel and beneficial idea [8]. Bidabadi et al. [9, 10] studied different properties of Lycopodium fuels to be used in a combustion chamber. Rahbari et al. [11] investigated the behavior of organic fuels dust cloud to achieve higher combustion efficiency. In addition to organic fuels, using clean energy such as solar energy [12, 13] and wind energy [14, 15] is a selective option for researchers to reduce environmental pollutions. Akbari et al. [16] used exergy analysis for a solar power plant. The authors concluded that maximum exergy destruction occurs in the collector. Farahbod et al. [17] studied a solar desalination unit. In this experimental research, they made freshwater and more concentrated brine by entering the brine into the system. Cıkkalp et al. [18, 19] analyzed a building heating system with an advanced exergy analysis. Yilanli et al. [20] investigated changes in the flow and energy of fuel for an aircraft using energy and exergy analyses. They concluded that exergy destruction depends on the state of flight. OzelErol et al. [21] studied the performance of an ice rink refrigeration system using advanced exergy analysis. The authors showed that 47.15% of the total loss of the system is avoidable, while 22.89% of the total exergy loss is exogenous. Ekici et al. [22] analyzed first and second thermodynamic laws for a turboprop with a mixture of fuel, including methanol and kerosene. Yasin et al. [23] studied the performance of a gas turbine with an advanced exergy method. The results showed 81.83% of exergy destruction was endogenous. Acikkalp et al. [24, 25], in two separate studies, performed advanced exergoenvironmental on a building. They concluded that the exogenous environmental effect of the system is 68.6%. Acikkalp et al. [26] investigated energy and exergy assessment of an air separator. The results showed that exergy and energy efficiency was 45.3% and 13.1%, respectively. Acikkalp et al. [27, 28] investigated an advanced exergy method for a trigeneration system. They concluded that exergy efficiency and total exergoeconomic factor were 0.354 and 0.069, respectively. Acikkalp performed thermodynamic analysis [29], environmental analysis [30], and economic analysis [31] for an electricity generating facility. The results showed that exergy efficiency, exergoenvironmental factor, and exergoeconomic factor were 0.402, 0.277, and 0.247, respectively. Kaushik et al. [32] estimated chemical exergy of solid, liquid, and gas fuels that were conventionally used in thermal power plants. They concluded that with increasing the amount of moisture in the fuel, chemical exergy decreases. Sheshpoli et al. [33] performed a thermodynamic analysis of waste heat recovery using the ORC cycle (organic Rankine cycle). They concluded that among the organic fluids, the R-134a has the maximum output power. Ghoreishi et al. [34] modeled six refrigerants for four ORC arrangements by EES software. Ksepko et al. [35] used effluent as an oxygen carrier in energy production processes. Lee et al. [36] added a brine treatment plant

to a CHP system and performed economic and exergy analyses on the system. They used a genetic algorithm to optimize thermo-economic and environmental objective functions. It was found that the total cost and the environmental harmful impacts reduced by 16.9% and 5.3%, respectively. Providing distilled water for a domestic building without harmful environmental effects was studied by Audah et al. [37]. They employed a new system that absorbed the moisture of the air to supply the water demand of a dwelling building. Employing the ZLD system for brine management in the coal industry in China was investigated by Xiong and Wei [38]. After a fast evaluation of the chemical industry of coal in China, the authors concluded that installing the ZLD system in this industry was declared as an obligation. Feasibility study of employing the process of the ZLD for dyeing wastewater treatment was done by Yao [39]. In this study, the impacts of the parameters, such as recovery ratio and consumption power on the operation of the system, were discussed. It was concluded that employing this system recovers 97% of the water in the waste stream.

Brine management is one of the global challenges that need to be studied precisely to reach sustainable aims. Demirbas [40] evaluated brine management and waste transfer processes. In this study, the definition of brine management, its categories, and brine management methods have been evaluated. Brine types have been grouped as commercial brine, biomedical brine, domestic brine, and dangerous brine. The study concluded that the best way for using solid wastes was by employing a composing-based method in which wastes were decomposed using natural biological improvements. Johannsen et al. [41] presented the benefits of high-pressure reverse osmosis toward ZLD in different operations.

The amount of blowdown in power plants makes lots of water and heat loss [42]. Therefore, the great amounts of water and energy losses are recovered in water and energy recovery. Ifaei et al. [43, 44] provided two schematics for reducing water blowdown in steam power plants. They added vapor compressor and absorption heat pump to a Rankine cycle and employed exergy–environmental analysis on the suggested system and drew a comparison between the aforementioned systems.

Akbari et al. [45] added a water and heat recovery to a solar thermal power plant. In this study, the authors investigated the impact of blowdown recovery on the net generated work by energy and exergy analyses on the power plant. The results showed that with water and heat recovery of the power plant blowdown, the generated work increased by 0.53% and drained wastewater reduced by 42%. Wang et al. [46] studied on an advanced wastewater recovery technology to extract latent heat of water vapor from flue gas in a steam power plant. They concluded that

recovered water can be used as makeup water in the boiler. Seigworth et al. [47] combined a ZLD membrane and MED desalination processes to minimize the cost. In this system, it was suggested that the total cost of the system can be decreased by 680$/day. In further studies, Petrov et al. [48] omitted selenium from FGD wastewater of a coal power plant. A few researchers implemented lost heat of the exhausted hot boiler's flue gas in fossil fuel power plants by desulfurization wastewater evaporation [49]. However, employing technologies such as spray drying technology in desulfurization is more practical in industry. Furthermore, lots of researchers worked on droplet evaporation principle in the drying process; however, due to hardness in precise observation in evaporation of drops, most of these studies were done numerically [50, 51].

The brine of a steam power plant is mostly consisting of the boiler blowdown and the feed water treatment brine with a much lower figure in comparison with the blowdown. Since the brine streams have reverse impacts on the immediate environment, taking the whole advantages of brines leads to eliminate these negative effects and to yield toward sustainable development. A novel ideal notion recognized by zero liquid discharge (ZLD) exploits the liquid discharge wherever possible for the aforementioned aims. Though there reviewed lots of researches on wastewater treatments, it is felt a gap in applying ZLD notion on a steam power plant to remove any brine discharges. This study aims to apply zero liquid discharge in a steam power plant using vacuum evaporator and study some key operating parameters' effects on the freshwater flow rate, power consumption, and exergy efficiency of the system within the different working cycles. The advantage of using this novel system is that water evaporating is done by high-temperature stream after roots pump and does not require an external heater. Moreover, the brine is evaporated in the vacuum environment; therefore, the boiling temperature of the liquid effluent is low, leading to a reduction in the consumed energy. This paper is followed by a system description, mathematical modeling and exergy analysis in third and fourth sections, respectively. Discussion on the results is given in the fifth section followed by the conclusion in the final section.

System description

In this study, mathematical modeling and energy and exergy analyses of ZLD system for recovering freshwater and heat of the brine are performed. The positioning of the system in the steam power plant is shown in Fig. 1. As the figure illustrates, blowdown of the power plant and the brine of the desalination feed water are entered into the
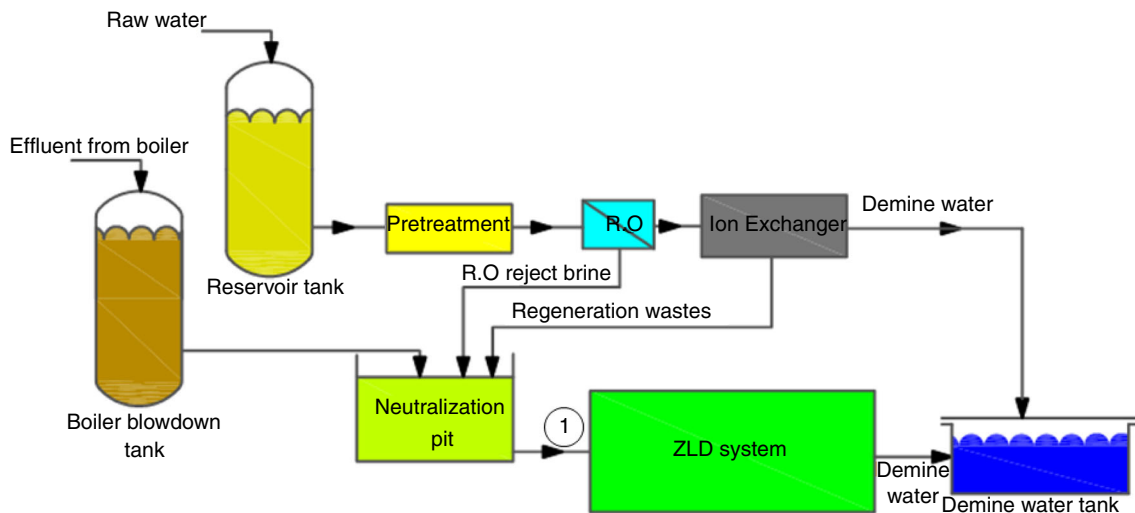
Fig. 1 Using the ZLD system in a steam power plant

ZLD system and the contained freshwater of the brine is entered into the storage tank.

The operation specifications of the ZLD system are shown in Fig. 2. Brine is entered into a vacuum evaporator, and by starting roots pump, the evaporator boiler pressure is decreased. As a consequence, the brine in the tank reaches its saturation point. In this situation, the contained water starts to evaporate and by passing through the roots pump, its temperature and pressure start to rise. By raising the temperature and pressure, the generated steam enters into a heat exchanger. In this heat exchanger, the steam gives its heat to the wastewater which is entering heat exchanger by a circulation pump.
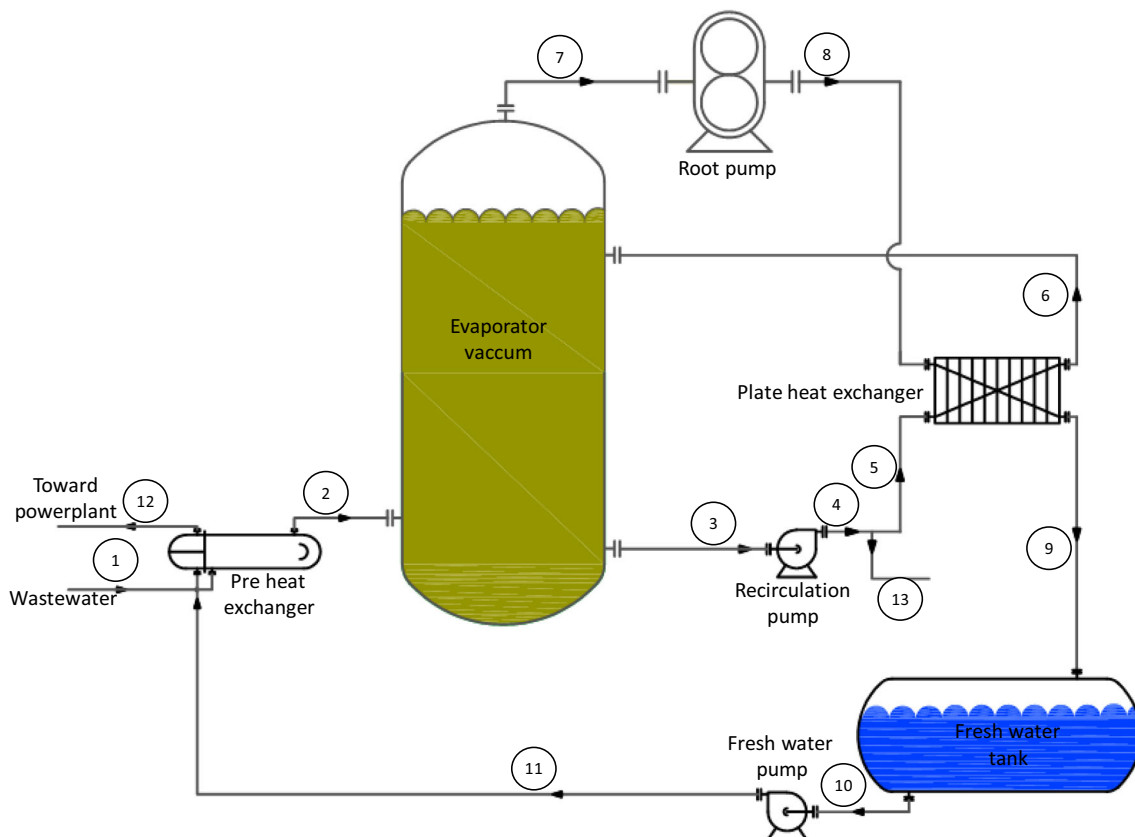

Fig. 2 Schematic of the ZLD system operation

By passing the heat exchanger, the enthalpy of wastewater rises and some of its contained water evaporates. This new steam gets into the roots pump again and the cycle goes on. The impact of the needed time for evaporating total freshwater in the evaporator boiler on the flow rate of the produced steam and generated power is shown in Figs. 3 and 4. In Figs. 5–16, the impact of the increasing volume of vacuum evaporator on different objective functions for the same evaporating time, which is taken 2 h, is analyzed. The main parts of the system are the evaporator boiler, roots pump, circulation pump, and heat exchanger. In each cycle, some amount of freshwater of brine in the vacuum evaporator is evaporated and in the end cycles, the freshwater of brine tends to be zero and a solution with high concentration is obtained that is drained out by the circulation pump.

Mathematical modeling

In this section, the mathematical modeling of the system is expressed.

The first step in the system modeling is energy analysis [52, 53]. All of the parts are assumed to be adiabatic; therefore, there will be no energy loss in them. For each part, energy and mass balances are written. The essential equations for mass and energy balances in the steady state are:

$$\sum_{i=1}^{n} \dot{m}_o = \sum_{i=1}^{n} \dot{m}_i \tag{1}$$

$$\dot{Q} - \dot{W} = \sum_{i=1}^{n} \dot{m}_o h_o - \sum_{i=1}^{n} \dot{m}_i h_i. \tag{2}$$

Evaporator boiler

At first, the wastewater is entered into the evaporator boiler, and after filling it, the entrance valve is closed. In this situation, the energy equation is:

$$\frac{\partial Q}{\partial t} - \frac{\partial W}{\partial t} = \dot{m}_o h_o - \dot{m}_i h_i + mc \frac{\partial T}{\partial t}. \tag{3}$$

When roots pump is being turned on, pressure in evaporator boiler is decreased to its saturation point. In this situation, as the system needed, heat is supplied by the roots pump and the amount of generated steam in the evaporator boiler in continuous cycles gets more and more, and the energy equation for vacuum evaporator is:

$$\dot{m}_3 h_3 + \dot{m}_7 h_7 = \dot{m}_6 h_6. \tag{4}$$

The amount of wastewater that is brined in point 13 is a function of entrance wastewater to the evaporator boiler. For evaluating flow rate, salinity balance is written as below:

$$X_1 \times \dot{m}_1 = \dot{m}_7 \times X_7 + \dot{m}_{13} \times X_{13}. \tag{5}$$

In Eq. (6), X_7 and X_{13} are assumed to be equal to zero and close to one, respectively.

Roots pump

By entering the steam into the roots pump and increasing the pressure and temperature of the steam, energy equation for this part is written as below:

$$\dot{m}_7 h_7 + \dot{W}_{RP} = \dot{m}_8 h_8 \tag{6}$$

$$\eta_{RP,is} = \frac{h_7 - h_{8,is}}{h_7 - h_8}. \tag{7}$$

In the above equation, $\eta_{RP,is}$ is the isentropic efficiency of the roots pump that is assumed to be 0.8.
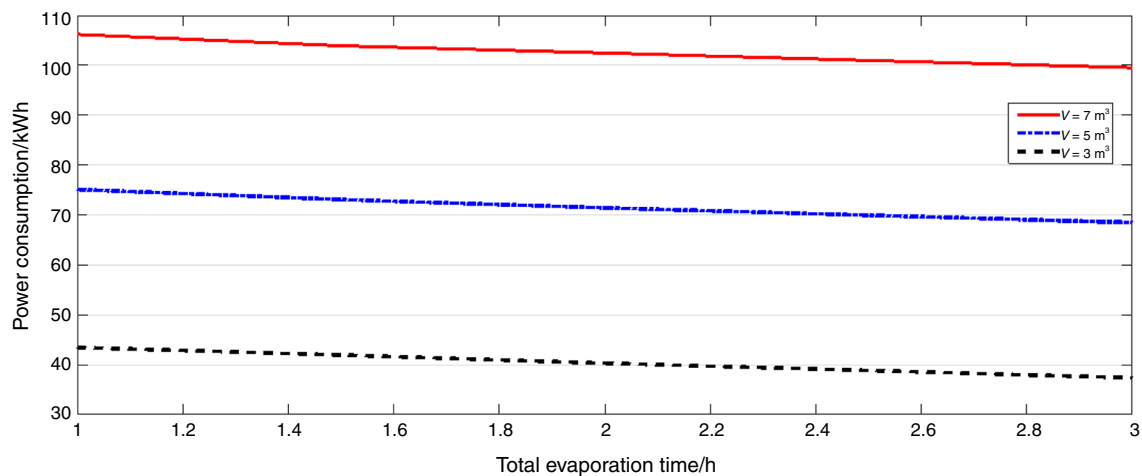

Fig. 3 Impact of total evaporation time on consumption power of ZLD system in different volumes of vacuum evaporator
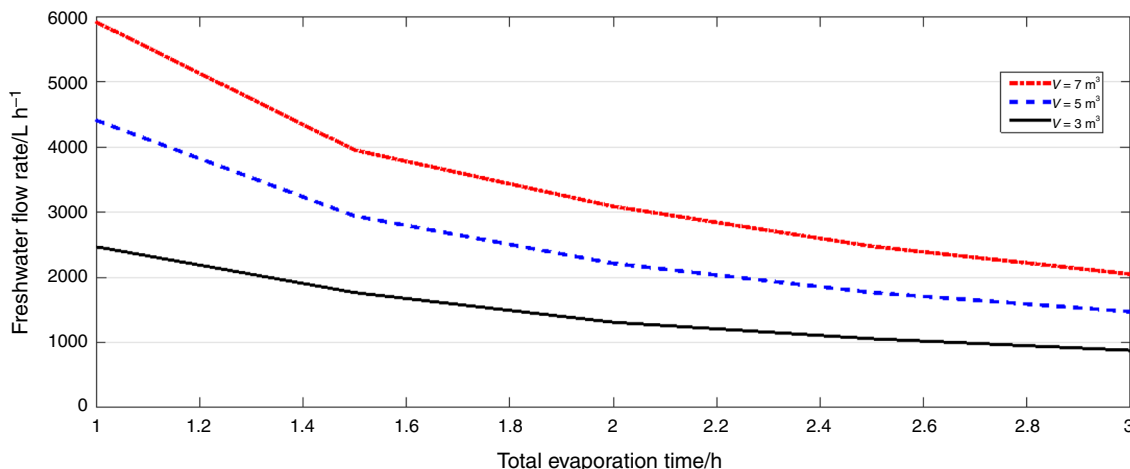
Fig. 4 Impact of total evaporating time on generated freshwater flow rate in different volumes of vacuum evaporator
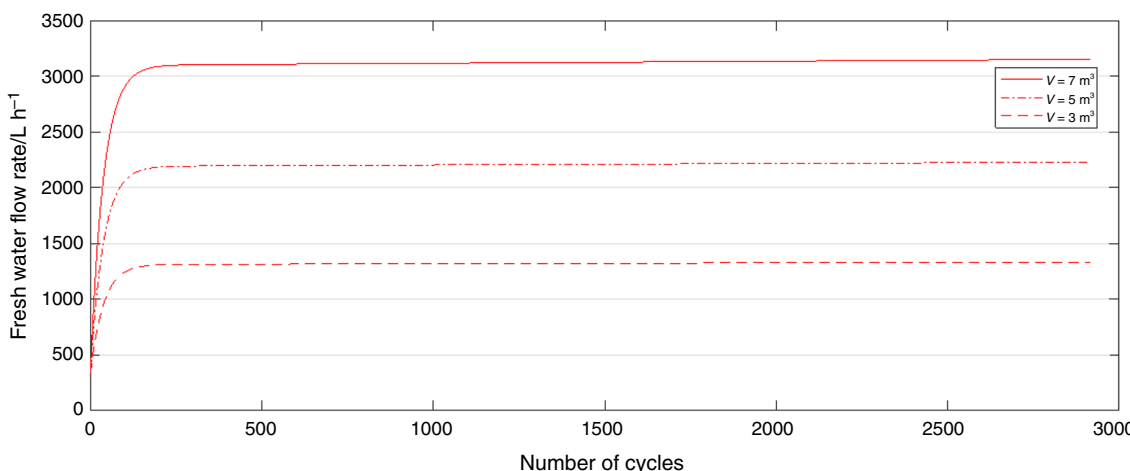

Fig. 5 Generated freshwater flow rate in different cycles in different volumes of vacuum evaporator

By using the above formula, the consumption power by the roots pump is written as below:

$$\dot{W}_{RP,i} = \dot{m}_{7,i}(h_7 - h_8) \tag{8}$$

In the above equation, $\dot{m}_{7,i}$ and $\dot{W}_{RP,i}$ are generated steam flow rate and consumed roots pump work in the ith cycle, respectively.

The total consumption power by the roots pump is the summation of consumption power in each cycle:

$$\dot{W}_{RP,tot} = \sum_{i=1}^{n} \dot{W}_{RP,i}. \tag{9}$$

Heat exchanger

By entering high-pressure and high-temperature steam from the one side and wastewater from the other side, the temperature of the steam will be decreased and is drained in the saturated point. In the heat exchanger, some amount of wastewater absorbs heat and is evaporated in each cycle. The amount of generated steam gets more and more in each cycle.

$$\dot{m}_8 h_8 + \dot{m}_5 h_5 = \dot{m}_6 h_6 + \dot{m}_9 h_9 \tag{10}$$

$$\dot{m}_8 = \dot{m}_9 \tag{11}$$

$$\dot{m}_4 = \dot{m}_6. \tag{12}$$

Circulation pump

For pumping the wastewater into the heat exchanger, a circulation pump is employed. The energy equation is written as:

$$\dot{m}_3 h_3 = \dot{m}_4 h_4 \tag{13}$$

$$\eta_{CP,is} = \frac{h_3 - h_{4,is}}{h_3 - h_4}. \tag{14}$$

In the above equation, $\eta_{CP,is}$ is the isentropic efficiency of the circulation pump, which is assumed to be 0.85.

By employing the above formula, consumption power of the circulation pump in each cycle is calculated as:

$$W_{CP,i} = \dot{m}_{3,i}(h_3 - h_4). \tag{15}$$

The total consumed work by the circulation pump is the summation of consuming work in each cycle:

$$W_{CP,tot} = \sum_{i=1}^{n} W_{CP,i}. \tag{16}$$

Distillate pump

By condensed steam in the heat exchanger, water is generated and stored in distillate tank; afterward, it is pumped by the distillate pump. The energy equation is written as:

$$\dot{m}_{10}h_{10} = \dot{m}_{11}h_{11} \tag{17}$$

$$\eta_{DP,is} = \frac{h_{10} - h_{11,is}}{h_{10} - h_{11}}. \tag{18}$$

The consumption power of the distillate pump is calculated as:

$$W_{DP} = \dot{m}_{10}(h_{10} - h_{11}). \tag{19}$$

The whole consumed work is obtained by summing the work of the roots pump, circulation pump, and distillate pump:

$$W_{tot} = \sum_{i=1}^{n} \left(W_{RP,i} + W_{CP,i} \right) + W_{DP}. \tag{20}$$

Preheat heat exchanger

By draining water from the distillate pump, its temperature gets more than generated wastewater of industries. Therefore, by using a heat exchanger, the temperature of the wastewater, before entering into the evaporator boiler, gets increased:

$$\dot{m}_1 h_1 + \dot{m}_{11}h_{11} = \dot{m}_{12}h_{12} + \dot{m}_2 h_2 \tag{21}$$

$$\dot{m}_1 = \dot{m}_2 \tag{22}$$

$$\dot{m}_{11} = \dot{m}_{12}. \tag{23}$$

Exergy analysis

Exergy is the maximum available work of a specified amount of energy to reach the ambient situation [54]. In the steady-state condition, the exergy balance of a control volume is written as [55, 56]:

$$\sum_j \left(1 - \frac{T_0}{T_j} \right) \dot{Q}_{CV} + \sum_i \dot{m}_i e_i - \sum_e \dot{m}_e e_e + \dot{W}_{CV} - \dot{E}_D$$
$$= 0. \tag{24}$$

The first term at the left side of the exergy equation is the heat exchanged between control volume and surrounding. The second and the third terms are inlet and outlet exergy of the control volume by flow rate of $\dot{m}$, respectively. The fourth term is the inlet work to the control volume. The last term is exergy destruction, which shows the irreversibility of processes in the control volume. In the above formula, e is the specific exergy that is the summation of kinetic, potential, physical, and chemical exergies:

$$e = e_{ke} + e_{po} + e_{ph} + e_{ch}. \tag{25}$$

Normally, the first two terms can be neglected [57, 58]. Physical specific exergy is the maximum available work of a system, in which the initial pressure and temperature of system P and T get the ambient ones P_0 and T_0:

$$e_{ph} = (h - h_0) - T_0(s - s_0). \tag{26}$$

In this situation, h and s are enthalpy and entropy of the system at temperature T and pressure P, while h_0 and s_0 are the enthalpy and entropy of the system at ambient pressure and temperature.

Chemical exergy is calculated as below:

$$e_{ch} = \sum_{j=1}^{N} y_j e_j^{ch} + RT_0 \left(\sum_{i=1}^{N} y_i \ln(y_i) \right). \tag{27}$$

Chemical exergy is defined normally for fuels [59]. There is no fuel in this case. Therefore, this kind of exergy is neglected here.

By employing Eqs. 24–27, the exergy destruction can be calculated. Table 1 provides the exergy destruction of each part.

Results and discussion

For exergy and energy analyses, the system is modeled by MATLAB^{TM} and the thermodynamic properties of the fluid are calculated by REFPROP [60]. Exergy is evaluated using thermodynamic equations for each stream. The volume of vacuum evaporator is an important parameter affecting the overall performance of the system. This value should be specified as input data in the proposed model. As discussed earlier, the process of evaporation is a batch process and is completed by some number of evaporation working cycles. Therefore, time is another key parameter in this simulation. Evaporation time is the total time

Table 1 Exergy destruction of each part of the system

Component	Exergy destruction	Exergy efficiency
Evaporator vacuum	$\dot{E}_{\mathrm{D}}^{\mathrm{EV}} = \sum \dot{E}_{\mathrm{in}} - \sum \dot{E}_{\mathrm{out}}$	$\eta_{\mathrm{ex}} = 1 - \dfrac{\dot{E}_{\mathrm{D}}^{\mathrm{EV}}}{\sum \dot{E}_{\mathrm{in}}}$
Roots pump	$\dot{E}_{\mathrm{D}}^{\mathrm{RP}} = \sum \dot{E}_{\mathrm{in}} - \sum \dot{E}_{\mathrm{out}} + \dot{W}_{\mathrm{in}}$	$\eta_{\mathrm{ex}} = 1 - \dfrac{\dot{E}_{\mathrm{D}}^{\mathrm{RP}}}{\sum \dot{E}_{\mathrm{in}} + W_{\mathrm{in}}}$
Heat exchanger	$\dot{E}_{\mathrm{D}}^{\mathrm{HX}} = \sum \dot{E}_{\mathrm{in}} - \sum \dot{E}_{\mathrm{out}}$	$\eta_{\mathrm{ex}} = 1 - \dfrac{\dot{E}_{\mathrm{D}}^{\mathrm{HX}}}{\sum \dot{E}_{\mathrm{in}}}$
Circulation pump	$\dot{E}_{\mathrm{D}}^{\mathrm{CP}} = \sum \dot{E}_{\mathrm{in}} - \sum \dot{E}_{\mathrm{out}} + \dot{W}_{\mathrm{in}}$	$\eta_{\mathrm{ex}} = 1 - \dfrac{\dot{E}_{\mathrm{D}}^{\mathrm{CP}}}{\dot{W}_{\mathrm{in}}}$
Distillate pump	$\dot{E}_{\mathrm{D}}^{\mathrm{DP}} = \sum \dot{E}_{\mathrm{in}} - \sum \dot{E}_{\mathrm{out}} + \dot{W}_{\mathrm{in}}$	$\eta_{\mathrm{ex}} = 1 - \dfrac{\dot{E}_{\mathrm{D}}^{\mathrm{DP}}}{\sum \dot{E}_{\mathrm{in}} + \dot{W}_{\mathrm{in}}}$
Preheat heat exchanger	$\dot{E}_{\mathrm{D}}^{\mathrm{PHX}} = \sum \dot{E}_{\mathrm{in}} - \sum \dot{E}_{\mathrm{out}}$	$\eta_{\mathrm{ex}} = 1 - \dfrac{\dot{E}_{\mathrm{D}}^{\mathrm{PHX}}}{\sum \dot{E}_{\mathrm{in}}}$

required for a batch evaporation process to be completed from the beginning of the first evaporation cycle to the end of the last evaporation cycle. In the following figures, symbol "V" stands for vacuum evaporator volume.

As illustrated in Fig. 3, the freshwater flow rate decreases by increasing evaporation time for a fixed amount of vacuum evaporator volume. Since the total freshwater volume is proportional to vacuum evaporator volume, freshwater flow rate is the sum of produced water in each individual cycle. Therefore, in a fixed vacuum evaporator volume, by increasing the evaporation time, freshwater flow rate will be reduced.

As it is shown in Fig. 4, with a fixed vacuum evaporator volume, by increasing the total evaporation time, the total consumption power of the system decreases. More evaporation time means that the wastewater in the vacuum evaporator needs more time to transfer to freshwater, which is constant as the volume of vacuum evaporator, and the generated steam flow rate decreases. On the other hand, since a large percentage of the power consumption of the ZLD system is consumed by the roots pump, a decrease in generated steam flow rate, which is volume flow rate through the roots pump, leads to a reduction in the consumption power of the roots pump. Therefore, the total consumption power of the ZLD system is decreased.

Since the recirculation flow rate and the distillate flow rate are constant, the consumed total power of the system is decreased. In addition, by increasing vacuum evaporator volume in constant time, the consumption power and freshwater flow rate are increased.

In Fig. 5, the amount of freshwater generation in each cycle for different volumes of vacuum evaporator is illustrated.

It is assumed that the required time for freshwater generation from the wastewater in the vacuum evaporator is constant for different volumes. Initially, by starting the roots pump, a relative vacuum is generated in the vacuum evaporator and the wastewater evaporation starts. As Fig. 5 shows, the amount of evaporated water in each cycle gets more and more, since at first by starting roots pump, the pressure of the vacuum evaporator decreases and reaches its saturation pressure and steam is generated. By passing generated steam from the roots pump, its temperature and pressure get increased and by giving its heat to the recirculating wastewater in the heat exchanger, some amount of wastewater vaporizes. The amount of generated steam in this process is more than the generated steam in the first cycle. Passing the generated steam from the roots pump, its temperature and pressure get higher, and since the steam flow rate in the second cycle is more than the first cycle, the heat exchanger transfers more heat to the recirculating wastewater that leads to more steam generation in the third cycle. Therefore, the generated steam flow rate gets higher through time. In Fig. 6, the average generated flow rate in different concentrations of wastewater in the evaporator is shown. In each cycle of this system, some amount of steam is generated and as time goes on, the level of wastewater in the vacuum evaporator decreases. Due to the continuous evaporation from the evaporator, concentration of the remaining wastewater in the vacuum evaporator increases to reach a highly concentrated solution. Afterward, this solution is drained through a valve after the circulation pump (stream 13).

The amount of rejected wastewater is a function of inlet concentration of wastewater to the vacuum evaporator. As is obvious in Fig. 6, raising the concentration of wastewater, the amount of average generated steam decreases. In a constant volume and period of time for this process, there is a lower total flow rate of freshwater. Also, as shown in Fig. 6, when the vacuum evaporator volume increases, this flow rate gets higher. With increasing the volume of the evaporator in the same evaporation time, the consumption power of the system increases and the temperature of steam that passes through the roots pump gets higher. With increasing consumption power of the roots pump, the heat given to the recirculation wastewater rises and consequently leads to more water vaporization.
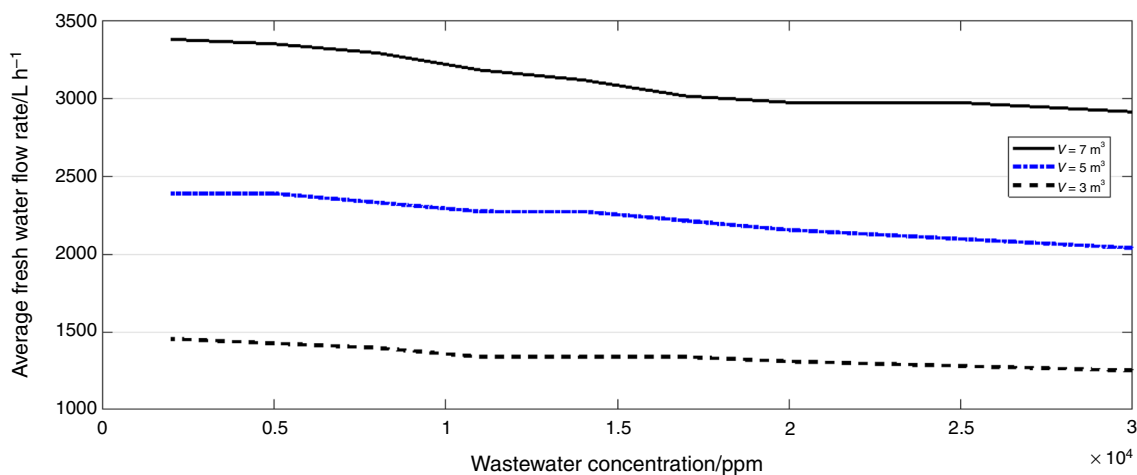
Fig. 6 Impact of inlet wastewater concentration to ZLD system on average flow rate of generated freshwater
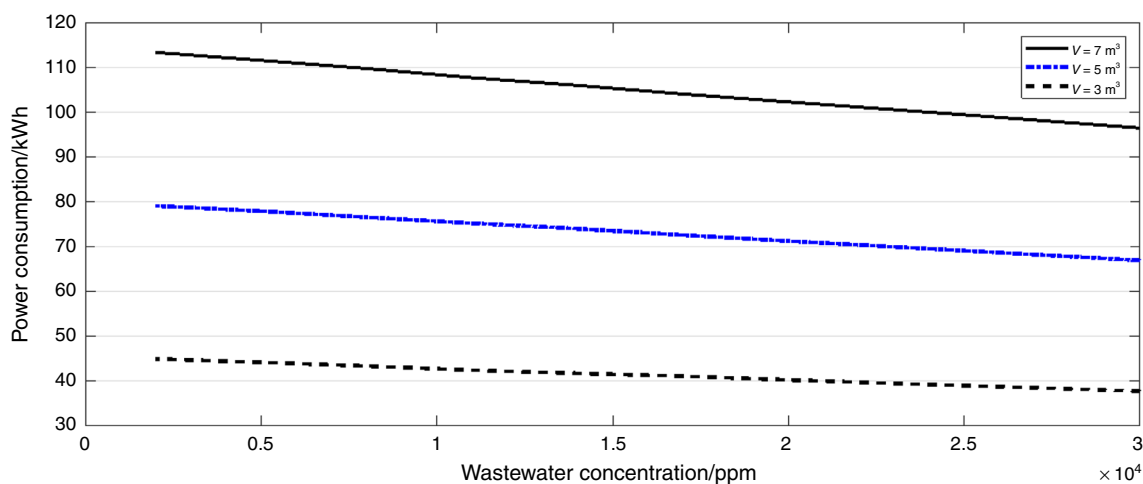

Fig. 7 Impact of concentration of inlet wastewater to ZLD system on total consumption power of the system

In Fig. 7, the impact of concentration of inlet wastewater on the consumption power of the system is shown.

By increasing the concentration of wastewater, the amount of consumption power decreases. This is due to a reduction in the amount of generated steam in the same volume as the concentration increases as illustrated in Fig. 6. Therefore, the passing flow rate from the roots pump is decreased, leading to a fall in the roots pump consumption power. On the other hand, recirculation and distillate flow rates are remained to be constant and the total consumption power decreases. In Figs. 8 and 9, the impact of the recirculation flow rate on the average flow rate of freshwater and the consumption power of the system is shown. In these figures, it is assumed that the evaporation time is constant.

As Fig. 8 illustrates, by increasing the recirculation flow rate, the average flow rate of generated freshwater is almost constant, since the evaporation time and the volume of evaporator vacuum stay constant. As a result, the average flow rate is independent of the recirculation flow rate.

Considering Fig. 9, it is a witness that in the constant evaporation time and increasing recirculation flow rate, the quality of the stream in point 6 is lessened; therefore, the enthalpy of inlet steam to the heat exchanger in point 8 reduces which causes a decrease in the consumption power of the roots pump. Since the consumption power of the roots pump is much more than the consumption power of the recirculation pump, decrease in the roots pump power results in a reduction in the power of the whole system.

In Fig. 10, the exergy efficiency of the main parts of the system is shown in different working cycles. It can be seen that in the initial cycles, the efficiency of exergy in the heat exchanger and roots pump is low and as time goes on, this efficiency rises to reach a constant level. In the evaporator, the efficiency of exergy in the initial cycles is high and this efficiency decreases, bottoming down as the time goes on. For recirculation pump, the exergy efficiency has a
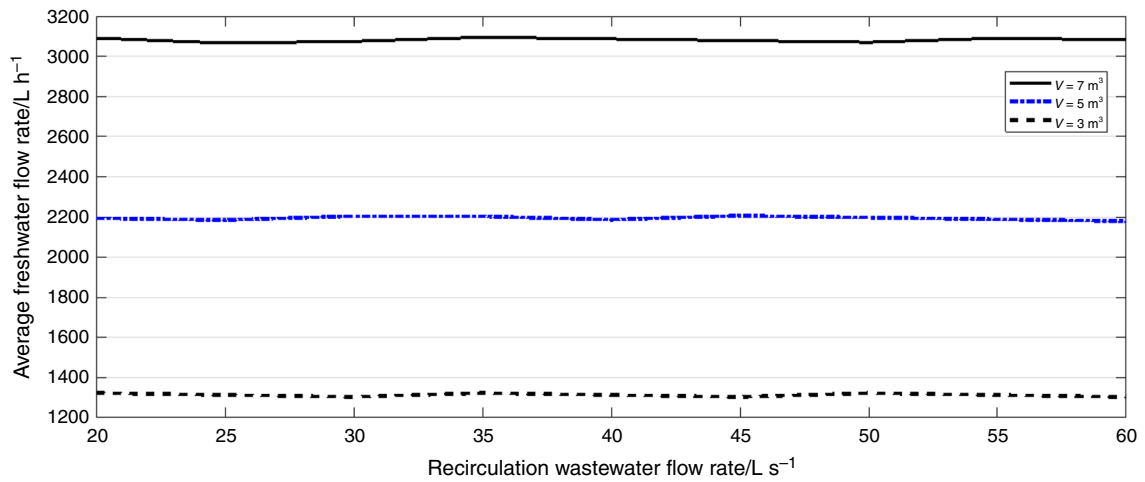
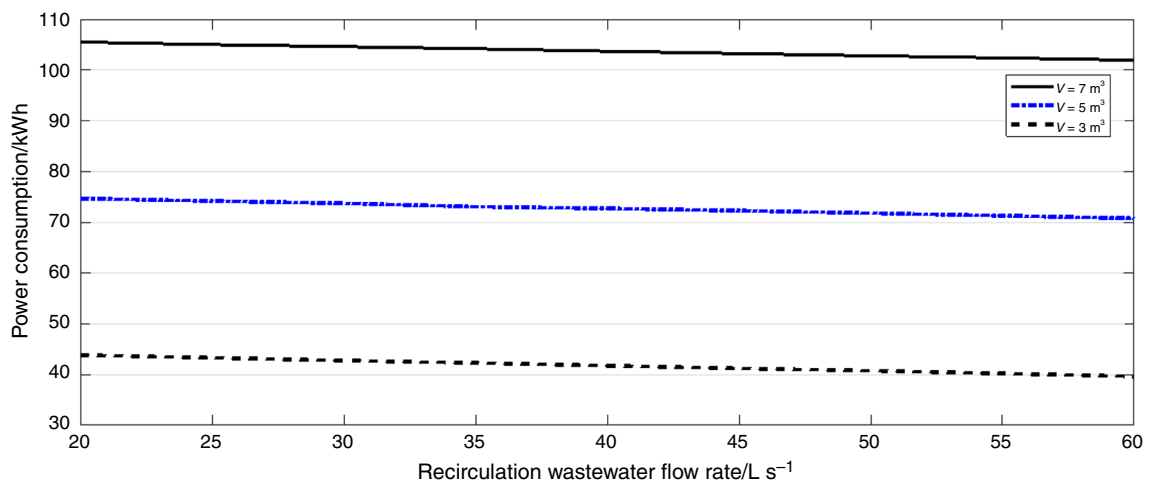**Fig. 8** Impact of recirculating wastewater flow rate on the generated freshwater flow rate

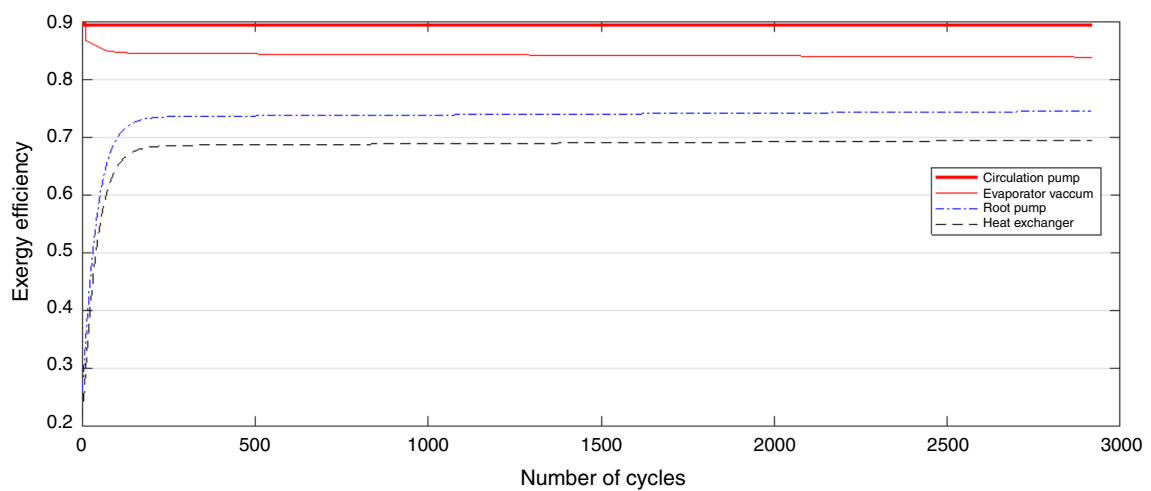**Fig. 9** Impact of recirculating wastewater flow rate on the consumption power of the system

Fig. 10 Exergy efficiency of main parts of the system in different cycles with $V = 3$ m^3

constant trend. The exergy efficiency for the components is calculated in Table 1. The increase in exergy efficiency of roots pump is as the result of the fact that in the initial cycles the amount of generated steam flow rate is low so that the temperature of steam after the roots pump gets high, and by raising the temperature, the entropy of the generated steam increases. Consequently, the exergy loss in the roots pump increases. The generated steam flow rate has the same trend as time goes on. Absorbing power by roots pump, its temperature decreases and the exergy loss decreases, unlike the exergy efficiency.

In the heat exchanger, inlet steam entropy is high in initial cycles that lead to a decrease in exergy of inlet flow to the heat exchanger. As a result, the exergy efficiency reduces. As time goes on, the steam flow rate increases. Therefore, the inlet exergy to heat exchanger gets more and exergy efficiency in heat exchanger increases. In the recirculating pump, due to the liquid phase of matter, the increased entropy of matter is not considerable; consequently, exergy loss is not much. The inlet fluid has also a constant temperature, so the inlet exergy stays constant. As a result, the exergy efficiency of this part has a constant trend. In the evaporator, in the initial cycles, the exergy loss to inlet exergy ratio is low; however, as time goes on and increases in generated steam flow rate this ratio gets more. Therefore, by considering the definition of exergy efficiency, this efficiency decreases during the time.

In Figs. 11 and 12, exergy efficiencies of the main parts are shown for higher volumes of the evaporator. It is assumed that the total evaporation time for different volumes of the evaporator is constant.

As it is obvious in the figure, by increasing the evaporator volume, the exergy efficiency of roots pump, heat exchanger, and evaporator decreases. By increasing evaporator volume, the generated steam flow rate gets increase

and rises the exergy loss to inlet exergy ratio for this part. By increasing this ratio, exergy efficiency of this part gets lower than exergy efficiency in lower volumes. But in the circulation pump, due to the liquid phase of passing fluid from this part, exergy loss and inlet exergy to the pump in different volumes almost remain constant. Therefore, in this part, by increasing evaporator volume, exergy efficiency stays constant.

In Fig. 13, changes in exergy efficiency for roots pump versus different concentrations of inlet wastewater in different volumes are shown. As Fig. 13 shows, by increasing concentration, the exergy efficiency of roots pump increases. Because by increasing wastewater concentration, more brine is rejected. Therefore, assuming that the required time for generation of freshwater from wastewater stays constant, exergy loss and consuming work of roots pump increase simultaneously. According to the definition of exergy efficiency for roots pump, exergy efficiency increases consequently.

In Fig. 14, the variations in exergy efficiency in heat exchanger versus different wastewater concentrations are shown. By the figure, increasing wastewater concentration leads to an increase in exergy efficiency. By increasing the wastewater concentration, consumption power of roots pump increases. Therefore, the exergy of steam before entering heat exchanger increases and with the constant exergy after the heat exchanger, the difference between inlet and outlet steam exergy increases. Consequently, according to the definition of exergy efficiency for heat exchangers, the exergy efficiency of this part increases.

Exergy efficiency of evaporator vacuum versus inlet wastewater concentration is analyzed in Fig. 15. By increasing wastewater concentration, the amount of brine increases. Since the total time for different concentrations is assumed to be constant, by increasing the concentration,
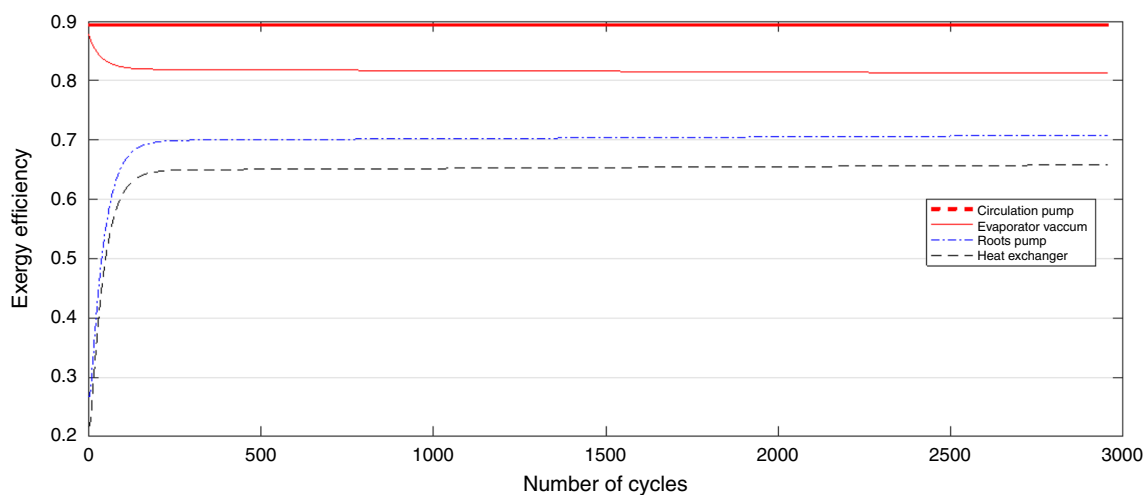

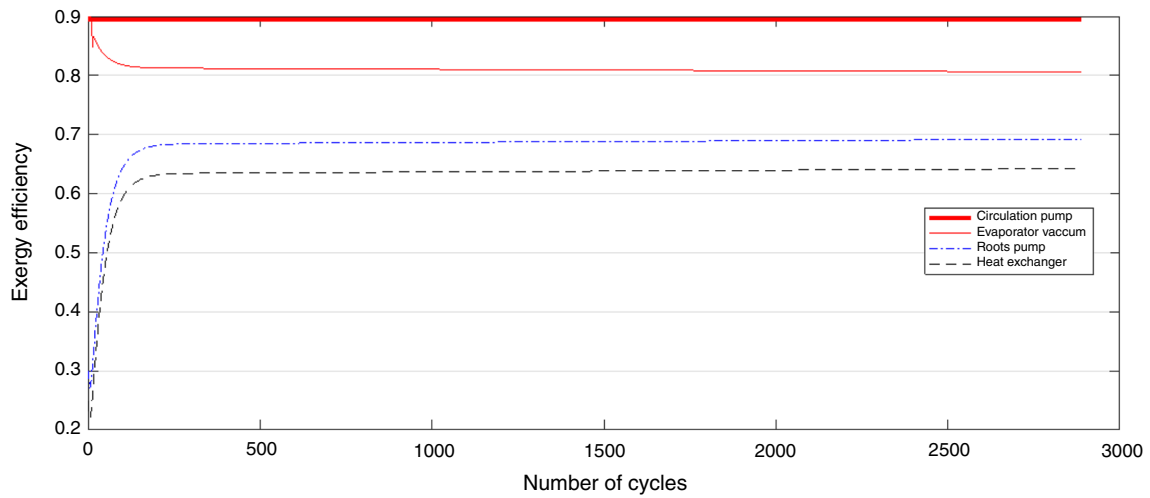**Fig. 11** Exergy efficiency of main parts of the system in different cycles with $V = 5$ m^3

Fig. 12 Exergy efficiency of main parts of the system in different cycles with $V = 7$ m^3
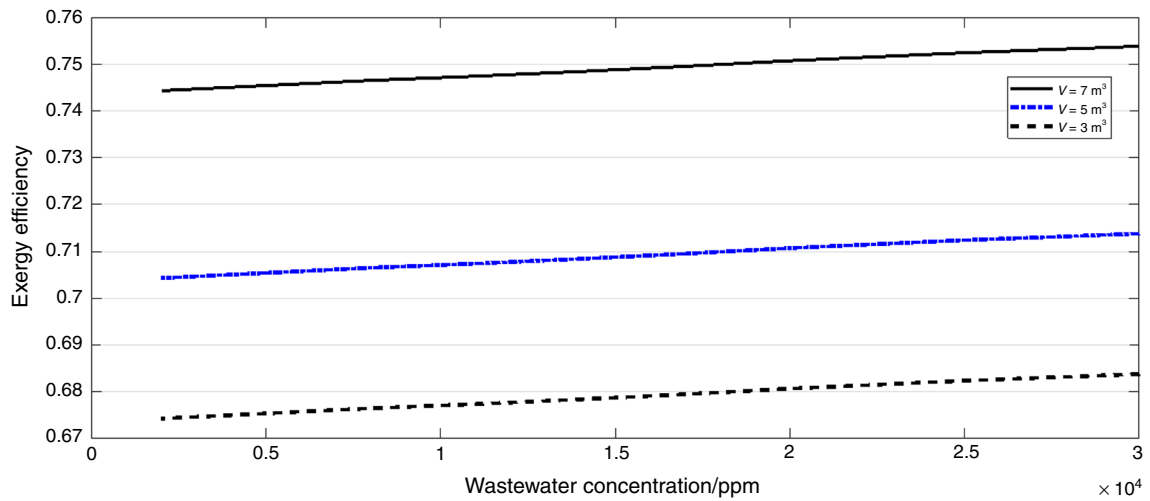

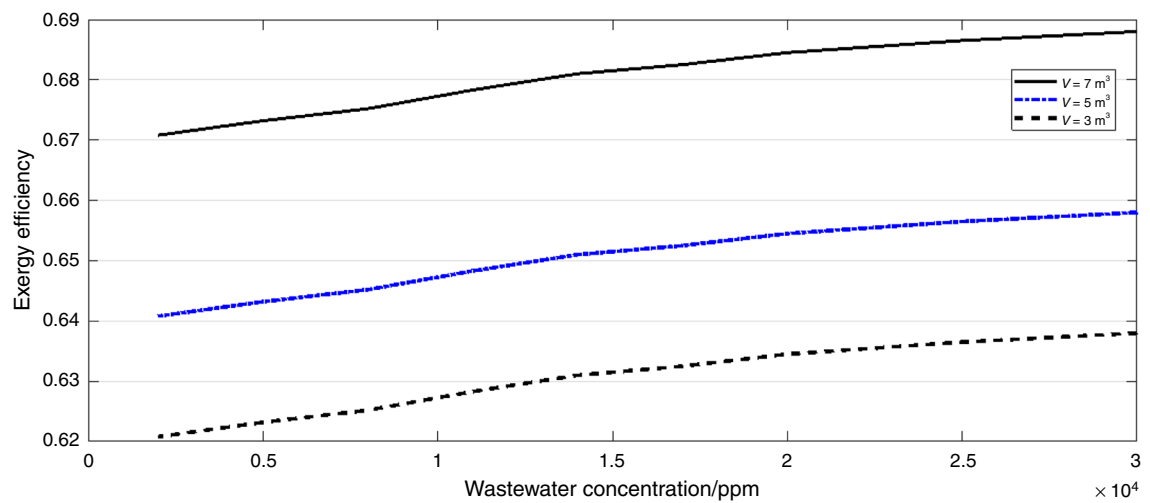**Fig. 13** Exergy efficiency of roots pump in different concentrations of wastewater

Fig. 14 Exergy efficiency of heat exchanger in different concentrations of wastewater
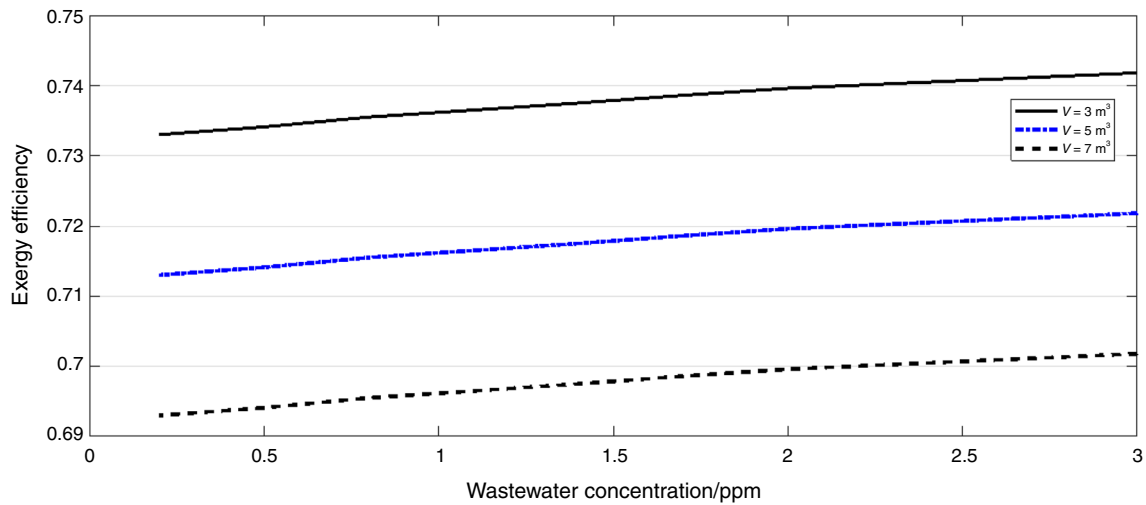
Fig. 15 Exergy efficiency of evaporator vacuum in different concentrations of wastewater
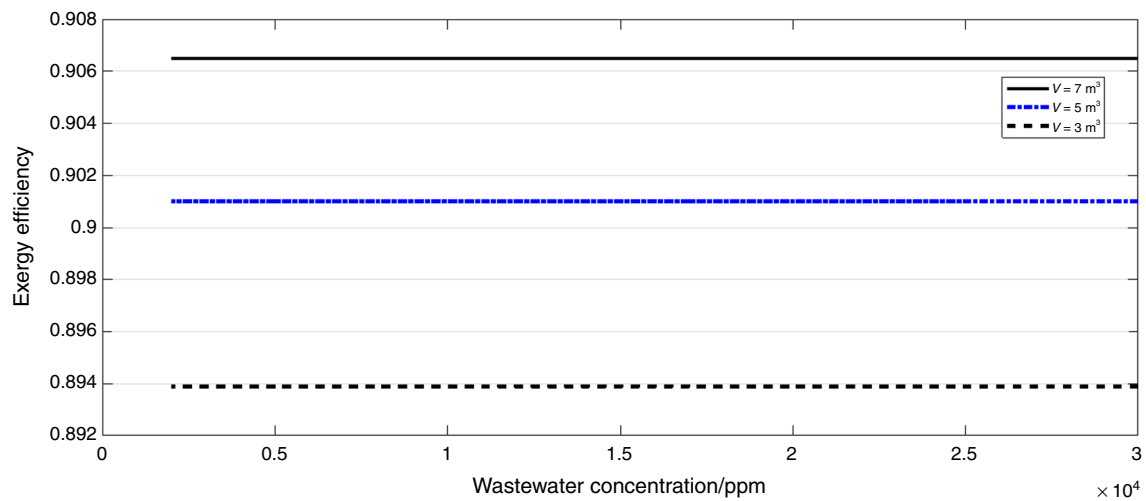

Fig. 16 Exergy efficiency of circulation pump in different concentrations of wastewater

the amount of water evaporation in the vacuum evaporator decreases. By decreasing the produced steam flow rate, the amount of heat given to the recirculation flow is reduced. Therefore, exergy of stream 6 is decreased and according to the definition of exergy efficiency for the evaporator boiler, exergy efficiency increases.

As shown in Fig. 16, exergy efficiency of circulation pump versus wastewater concentration is almost constant.

Inlet flow to the pump is in the liquid phase, and wastewater concentration does not affect any changes on the inlet flow of the pump. Therefore, by constant flow rate passing to the pump, power consumption of pump does not change, and as a result, because the power consumption of pump has a direct impact on the exergy efficiency, the exergy efficiency remains constant.

Conclusions

In this study, by modeling and exergy analyzing of a ZLD system, almost all of the contained water of blowdown is recovered as freshwater to the power plant. The advantage of using this novel system is that water evaporating is done by high-temperature stream after roots pump and does not require an external heater. Analyses are conducted for different volumes of vacuum evaporator. The results showed that the amount of generated freshwater increases by raising the volume in the same evaporation time. The concentration of blowdown in power plants is one of the main parameters in the blowdown treatment. By increasing the blowdown concentration, due to the less freshwater production, the power used by the system decreases. The impact of the blowdown concentration on the exergy

efficiency of each component of the system shows that by increasing the concentration to 30,000 ppm, in the situation that the volume of the evaporator vacuum is equal to 7 m^3, the exergy efficiency of roots pump, evaporator vacuum, and heat exchanger will be increased to 0.684, 0.702, and 0.639, respectively. It should be noted that the exergy efficiency of recirculation pumps in different wastewater concentration has a steady trend. Moreover, due to an increase in recirculation flow rate, consumption power of the system is decreased, but generated freshwater flow rate stays almost constant. Exergy efficiencies of the main parts within the system are calculated, and it is concluded that efficiencies of roots pump and heat exchanger increase as time goes on, and initially the slope of exergy efficiency changes for two specified parts, roots pump and heat exchanger, and decreases after a plateau. Exergy efficiency of recirculation pump remains almost constant, and exergy efficiency of vacuum evaporator decreases dramatically at the initial as time goes on and finally experiences a smooth decrease.

References

1. Di Fraia S, Massarotti N, Vanoli L. A novel energy assessment of urban wastewater treatment plants. Energy Convers Manag. 2018;163:304–13. https://doi.org/10.1016/J.ENCONMAN.2018.02.058.

2. Song J, Yang W, Li Z, Higano Y, Wang X. Discovering the energy, economic and environmental potentials of urban wastes: an input–output model for a metropolis case. Energy Convers Manag. 2016;114:168–79. https://doi.org/10.1016/J.ENCONMAN.2016.02.014.

3. Yang Y, Zhu J, Zhu G, Yang L, Zhu Y. The effect of high temperature on syngas production by immediate pyrolysis of wet sewage sludge with sawdust. J Therm Anal Calorim. 2018;132:1783–94. https://doi.org/10.1007/s10973-018-7143-9.

4. Naeimi A, Bidi M, Ahmadi MH, Kumar R, Sadeghzadeh M, Alhuyi Nazari M. Design and exergy analysis of waste heat recovery system and gas engine for power generation in Tehran cement factory. Therm Sci Eng Prog. 2019;9:299–307. https://doi.org/10.1016/j.tsep.2018.12.007.

5. Nakoa K, Rahaoui K, Date A, Akbarzadeh A. Sustainable Zero Liquid Discharge desalination (SZLDD). Sol Energy. 2016;135:337–47. https://doi.org/10.1016/J.SOLENER.2016.05.047.

6. Naseri A, Bidi M, Ahmadi M, Saidur R. Exergy analysis of a hydrogen and water production process by a solar-driven transcritical CO_2 power cycle with Stirling engine. J Clean Prod. 2017;158:165–81. https://doi.org/10.1016/J.JCLEPRO.2017.05.005.

7. Han D, He WF, Yue C, Pu WH. Study on desalination of zero-emission system based on mechanical vapor compression. Appl Energy. 2017;185:1490–6. https://doi.org/10.1016/J.APENERGY.2015.12.061.

8. Mohammadi A, Ashouri M, Ahmadi MH, Bidi M, Sadeghzadeh M, Ming T. Thermoeconomic analysis and multiobjective optimization of a combined gas turbine, steam, and organic Rankine cycle. Energy Sci Eng. 2018;6:506–22. https://doi.org/10.1002/ese3.227.

9. Bidabadi M, Akbari Vakilabadi M, Khoeini Poorfar A, Monteiro E, Rouboa A, Rahbari A. Mathematical modeling of premixed counterflow combustion of organic dust cloud. Renew Energy. 2016;92:376–84. https://doi.org/10.1016/J.RENENE.2016.02.002.

10. Bidabadi M, Vakilabadi MA, Esmaeilnejad A. Strain rate effect on microorganic dust flame in a premixed counterflow. Heat Transf Res. 2015;46:1–11. https://doi.org/10.1615/heattransres.2014005471.

11. Rahbari A, Wong K-F, Vakilabadi MA, Poorfar AK, Afzalabadi A. Theoretical investigation of particle behavior on flame propagation in lycopodium dust cloud. J Energy Resour Technol. 2016;139:12202–7.

12. Dabiri S, Khodabandeh E, Poorfar AK, Mashayekhi R, Toghraie D, Abadian Zade SA. Parametric investigation of thermal characteristic in trapezoidal cavity receiver for a linear Fresnel solar collector concentrator. Energy. 2018;153:17–26. https://doi.org/10.1016/J.ENERGY.2018.04.025.

13. Khodabandeh E, Safaei MR, Akbari S, Akbari OA, Alrashed AAAA. Application of nanofluid to improve the thermal performance of horizontal spiral coil utilized in solar ponds: geometric study. Renew Energy. 2018;122:1–16. https://doi.org/10.1016/J.RENENE.2018.01.023.

14. Ashrafi ZN, Ghasemian M, Shahrestani MI, Khodabandeh E, Sedaghat A. Evaluation of hydrogen production from harvesting wind energy at high altitudes in Iran by three extrapolating Weibull methods. Int J Hydr Energy. 2018;43:3110–32. https://doi.org/10.1016/J.IJHYDENE.2017.12.154.

15. Akbari Vakiabadi M, Bidi M. Technical and economical evaluation of grid-connected renewable power generation system for a residential urban area. Int J Low-Carbon Technol. 2019;14:1–13. https://doi.org/10.1093/ijlct/cty053.

16. Vakilabadi MA, Bidi M, Najafi AF, Ahmadi MH. Exergy analysis of a hybrid solar-fossil fuel power plant. Energy Sci Eng. 2019;7:146–61. https://doi.org/10.1002/ese3.265.

17. Farahbod F, Mowla D, Jafari Nasr MR, Soltanieh M. Experimental study of a solar desalination pond as second stage in proposed zero discharge desalination process. Sol Energy. 2013;97:138–46. https://doi.org/10.1016/J.SOLENER.2013.02.033.

18. Açıkkalp E, Hepbasli A, Yucer CT, Karakoc TH. Advanced life cycle integrated exergoeconomic analysis of building heating systems: an application and proposing new indices. J Clean Prod. 2018;195:851–60. https://doi.org/10.1016/J.JCLEPRO.2018.05.239.

19. Açıkkalp E, Yucer CT, Hepbasli A, Karakoc TH. Advanced low exergy (ADLOWEX) modeling and analysis of a building from the primary energy transformation to the environment. Energy Build. 2014;81:281–6. https://doi.org/10.1016/J.ENBUILD.2014.06.024.

20. Karakoc T, Açıkkalp E, Altuntaş Ö, Yilanli M. Aircraft fuel system energy and exergy analysis under hot day conditions. Int J Exergy. 2018;25:152. https://doi.org/10.1504/IJEX.2018.10010741.

21. Erol GO, Açıkkalp E, Hepbasli A. Performance assessment of an ice rink refrigeration system through advanced exergoeconomic analysis method. Energy Build. 2017;138:118–26. https://doi.org/10.1016/J.ENBUILD.2016.12.025.

22. Ekici S, Altuntaş Ö, Açıkkalp E, Söğut Z, Karakoc T. Assessment of thermodynamic performance and exergetic-sustainability of turboprop engine based on exergetic indicators using mixture of kerosene and methanol. Int J Exergy. 2015. https://doi.org/10.1504/ijex.2016.075666.

23. Şöhret Y, Açıkkalp E, Hepbasli A, Karakoc TH. Advanced exergy analysis of an aircraft gas turbine engine: splitting exergy

destructions into parts. Energy. 2015;90:1219–28. https://doi.org/10.1016/j.energy.2015.06.071.

24. Açıkkalp E, Hepbasli A, Yucer CT, Karakoc TH. Advanced exergoenvironmental assessment of a building from the primary energy transformation to the environment. Energy Build. 2015;89:1–8. https://doi.org/10.1016/J.ENBUILD.2014.12.020.

25. Açıkkalp E, Yucer CT, Hepbasli A, Karakoc TH. Advanced low exergoeconomic (ALEXERGO) assessment of a building along with its heating system at various stages. Energy Build. 2015;87:66–73. https://doi.org/10.1016/J.ENBUILD.2014.11.020.

26. Açıkkalp E, Yamık H, Caner N, Açıkkalp E. Energy and exergy evaluation of an air separation facility: a case study. Sep Sci Technol. 2014. https://doi.org/10.1080/01496395.2014.907316.

27. Açıkkalp E, Aras H, Hepbasli A. Advanced exergy analysis of a trigeneration system with a diesel-gas engine operating in a refrigerator plant building. Energy Build. 2014;80:268–75. https://doi.org/10.1016/j.enbuild.2014.05.029.

28. Açıkkalp E, Aras H, Hepbasli A. Advanced exergoeconomic analysis of a trigeneration system using a diesel-gas engine. Appl Therm Eng. 2014;67:388–95. https://doi.org/10.1016/j.applthermaleng.2014.03.005.

29. Açıkkalp E, Aras H, Hepbasli A. Advanced exergy analysis of an electricity-generating facility using natural gas. Energy Convers Manag. 2014;82:146–53. https://doi.org/10.1016/j.enconman.2014.03.006.

30. Açıkkalp E, Aras H, Hepbasli A. Advanced exergoenvironmental assessment of a natural gas-fired electricity generating facility. Energy Convers Manag. 2014;81:112–9. https://doi.org/10.1016/j.enconman.2014.02.011.

31. Açıkkalp E, Aras H, Hepbasli A. Advanced exergoeconomic analysis of an electricity-generating facility that operates with natural gas. Energy Convers Manag. 2014;78:452–60. https://doi.org/10.1016/j.enconman.2013.11.003.

32. Kaushik SC, Singh OK. Estimation of chemical exergy of solid, liquid and gaseous fuels used in thermal power plants. J Therm Anal Calorim. 2014;115:903–8. https://doi.org/10.1007/s10973-013-3323-9.

33. Sheshpoli MA, Ajarostaghi SSM, Delavar MA. Thermodynamic analysis of waste heat recovery from hybrid system of proton exchange membrane fuel cell and vapor compression refrigeration cycle by recuperative organic Rankine cycle. J Therm Anal Calorim. 2019;135:1699–712. https://doi.org/10.1007/s10973-018-7338-0.

34. Shams Ghoreishi SM, Akbari Vakilabadi M, Bidi M, Khoeini Poorfar A, Sadeghzadeh M, Ahmadi MH, et al. Analysis, economical and technical enhancement of an organic Rankine cycle recovering waste heat from an exhaust gas stream. Energy Sci Eng. 2019. https://doi.org/10.1002/ese3.274.

35. Ksepko E, Klimontko J, Kwiecinska A. Industrial wastewater treatment wastes used as oxygen carriers in energy generation processes. J Therm Anal Calorim. 2019. https://doi.org/10.1007/s10973-019-08214-8.

36. Lee S, Esfahani IJ, Ifaei P, Moya W, Yoo C. Thermo-environ-economic modeling and optimization of an integrated wastewater treatment plant with a combined heat and power generation system. Energy Convers Manag. 2017;142:385–401. https://doi.org/10.1016/J.ENCONMAN.2017.03.060.

37. Audah N, Ghaddar N, Ghali K. Optimized solar-powered liquid desiccant system to supply building fresh water and cooling needs. Appl Energy. 2011;88:3726–36. https://doi.org/10.1016/J.APENERGY.2011.04.028.

38. Xiong R, Wei C. Current status and technology trends of Zero Liquid Discharge at coal chemical industry in China. J Water Process Eng. 2017;19:346–51. https://doi.org/10.1016/J.JWPE.2017.09.005.

39. Yao J, Wen D, Shen J, Wang J. Zero discharge process for dyeing wastewater treatment. J Water Process Eng. 2016;11:98–103. https://doi.org/10.1016/J.JWPE.2016.03.012.

40. Demirbaş A. Biomass resource facilities and biomass conversion processing for fuels and chemicals. Energy Convers Manag. 2001;42:1357–78. https://doi.org/10.1016/S0196-8904(00)00137-0.

41. Johannsen P, Karlapudi R, Reinhold G. High pressure reverse osmosis for wastewater minimization and Zero Liquid Discharge applications. Desalination. 2006;199:84–5. https://doi.org/10.1016/j.desal.2006.03.021.

42. Ahmadi MH, Alhuyi Nazari M, Sadeghzadeh M, Pourfayaz F, Ghazvini M, Ming T, et al. Thermodynamic and economic analysis of performance evaluation of all the thermal power plants: a review. Energy Sci Eng. 2019;7:30–65. https://doi.org/10.1002/ese3.223.

43. Ifaei P, Ataei A, Yoo C. Thermoeconomic and environmental analyses of a low water consumption combined steam power plant and refrigeration chillers-Part 2: thermoeconomic and environmental analysis. Energy Convers Manag. 2016;123:625–42. https://doi.org/10.1016/J.ENCONMAN.2016.06.030.

44. Ifaei P, Rashidi J, Yoo C. Thermoeconomic and environmental analyses of a low water consumption combined steam power plant and refrigeration chillers—Part 1: energy and economic modelling and analysis. Energy Convers Manag. 2016;123:610–24. https://doi.org/10.1016/J.ENCONMAN.2016.06.036.

45. Akbari Vakilabadi M, Bidi M, Najafi AF. Energy, Exergy analysis and optimization of solar thermal power plant with adding heat and water recovery system. Energy Convers Manag. 2018;171:1639–50. https://doi.org/10.1016/J.ENCONMAN.2018.06.094.

46. Wang D, Bao A, Kunc W, Liss W. Coal power plant flue gas waste heat and water recovery. Appl Energy. 2012;91:341–8. https://doi.org/10.1016/J.APENERGY.2011.10.003.

47. Seigworth A, Ludlum R, Reahl E. Case study: integrating membrane processes with evaporation to achieve economical Zero Liquid Discharge at the Doswell Combined Cycle Facility. Desalination. 1995;102:81–6. https://doi.org/10.1016/0011-9164(95)00044-3.

48. Petrov P, Charters W, Wallschläger JD. Identification and determination of selenosulfate and selenocyanate in flue gas desulfurization waters. Environ Sci Technol. 2011;46:1716–23. https://doi.org/10.1021/es202529w.

49. Córdoba P. Status of flue gas desulphurisation (FGD) systems from coal-fired power plants: overview of the physic-chemical control processes of wet limestone FGDs. Fuel. 2015;144:274–86. https://doi.org/10.1016/J.FUEL.2014.12.065.

50. Barrow H, Pope CW. Droplet evaporation with reference to the effectiveness of water-mist cooling. Appl Energy. 2007;84:404–12. https://doi.org/10.1016/J.APENERGY.2006.09.007.

51. Chow LC, Chung JN. Evaporation of water into a laminar stream of air and superheated steam. Int J Heat Mass Transf. 1983;26:373–80. https://doi.org/10.1016/0017-9310(83)90041-8.

52. Ahmadi MH, Sameti M, Pourkiaei SM, Ming T, Pourfayaz F, Chamkha AJ, et al. Multi-objective performance optimization of irreversible molten carbonate fuel cell–Stirling heat engine–reverse osmosis and thermodynamic assessment with ecological objective approach. Energy Sci Eng. 2018;6:783–96. https://doi.org/10.1002/ese3.252.

53. Ahmadi MH, Jokar MA, Ming T, Feidt M, Pourfayaz F, Astaraei FR. Multi-objective performance optimization of irreversible molten carbonate fuel cell–Braysson heat engine and thermodynamic analysis with ecological objective approach. Energy. 2018;144:707–22. https://doi.org/10.1016/J.ENERGY.2017.12.028.

54. Kotas TJ, Tadeusz J. The exergy method of thermal plant analysis. London: Butterworths; 1985.

55. Ahmadi M, Sadaghiani SM, Pourfayaz F, Ghazvini M, Mahian O, Mehrpooya M, et al. Energy and exergy analyses of a solid oxide fuel cell-gas turbine-organic rankine cycle power plant with liquefied natural gas as heat sink. Entropy. 2018;20:484. https://doi.org/10.3390/e20070484.

56. Mohammadi A, Ahmadi MH, Bidi M, Ghazvini M, Ming T. Exergy and economic analyses of replacing feedwater heaters in a Rankine cycle with parabolic trough collectors. Energy Rep. 2018;4:243–51. https://doi.org/10.1016/J.EGYR.2018.03.001.

57. Kanoglu M, Dincer I, Rosen MA. Understanding energy and exergy efficiencies for improved energy management in power plants. Energy Pol. 2007;35:3967–78. https://doi.org/10.1016/J.ENPOL.2007.01.015.

58. Ameri M, Ahmadi P. The study of ambient temperature effects on exergy losses of a heat recovery steam generator. In: Proceedings of international conference on power engineering, Hang Zhou: 2007.

59. Vandani AMK, Bidi M, Ahmadi F. Exergy analysis and evolutionary optimization of boiler blowdown heat recovery in steam power plants. Energy Convers Manag. 2015;106:1–9. https://doi.org/10.1016/J.ENCONMAN.2015.09.018.

60. Lemmon EW, Huber ML, Mclinden MO. NIST reference fluid thermodynamic and transport properties—REFPROP 9.0. 2010.

Publisher's Note Springer Nature remains neutral with regard to jurisdictional claims in published maps and institutional affiliations.